Liquid Crystals
Publication details, including instructions for authors and subscription information:
http://www.informaworld.com/smpp/title~content=t713926090

Anchoring transitions of liquid crystals on SiO _x

Cheng Chen[a]; Philip J. Bos[a]; James E. Anderson[b]
[a] Liquid Crystal Institute, Kent State University, Kent, OH 44242, USA [b] HANA Microdisplay Technology Inc, Twinsburg, OH 44087, USA

To cite this Article Chen, Cheng , Bos, Philip J. and Anderson, James E.(2008) 'Anchoring transitions of liquid crystals on SiO _x ', Liquid Crystals, 35: 4, 465 — 481
To link to this Article: DOI: 10.1080/02678290801939244
URL: http://dx.doi.org/10.1080/02678290801939244

Liquid Crystals,
Vol. 35, No. 4, April 2008, 465–481

Taylor & Francis
Taylor & Francis Group

Anchoring transitions of liquid crystals on SiO_x

Cheng Chen[a], Philip J. Bos[a]* and James E. Anderson[b]

[a]*Liquid Crystal Institute, Kent State University, Kent, OH 44242, USA;* [b]*HANA Microdisplay Technology Inc, Twinsburg, OH 44087, USA*

(Received 19 November 2007; final form 23 January 2008)

Anchoring transitions were observed of nematic liquid crystal (LC) mixtures on obliquely evaporated SiO_x by varying the relative abundance of two components in the mixture. Of these two components, one has a longitudinal cyano group and another has lateral cyano groups. It was also found that both temperature and SiO_x thickness variations are able to shift the anchoring transitions. The anchoring on SiO_x has two origins: long-range van der Waals potential and short-range surface interactions. Since the two origins have opposite preference in LC director orientation the observed transition is caused by the change of their relative strength. Thermal absorption–desorption of molecules on SiO_x surface is important in determining the strength of short-range interactions, whereas the layer thickness and optical properties of SiO_x are dependent on the van der Waals potential. Based on previous work by de Gennes we propose a model to describe the observed phenomenon.

Keywords: anchoring transition; nematic LC; van der Waals potential; short-range interaction; silicon oxide alignment layer

1. Introduction

Obliquely evaporated silicon oxide (SiO_x) thin films have been of great interest in the past decades for their use as liquid crystal (LC) alignment layers. Compared to the traditional rubbed polyimides (PIs), SiO_x has unique advantages. It is obtained using a non-contact method that produces less cosmetic defects and particles that contaminate the alignment surface. It is also less sensitive to UV light and is capable of producing a wide range of pretilt angles. These advantages have caused SiO_x to be considered or implemented in applications like microdisplays and telecommunications devices. Along with the increased interest, have been efforts to understand the mechanism of the alignment. The following is a review of some work in that area.

Short-range interactions

Surface short-range interactions have been found important in LC alignment. For example, it was discovered that the SiO_x column structures that stick out from the surface are important for LC anchoring. So are the molecular groups on SiO_x further coated with alcohol, silane or other organic material. The surface has been pictured as a comb with LC molecules embedded between the molecular groups sticking out of the surface (*1–3*). Wen *et al.* (*4*) have reported an interesting alignment phenomenon observed on SiO_x and successfully explained it using this theory.

From a more chemical–physical point of view, some other researchers have demonstrated that the strong interfacial interactions between the surface and the contacting LC molecules give rise to the anchoring energy that determines the bulk orientation (*5, 6*). These interfacial interactions may include steric interaction, charge–charge interaction, charge–dipole interaction, dipole–dipole interaction, hydrogen bonding or even chemical bonding. Since LCs are often polar materials, the coupling between the permanent dipole of LC and the surface dipoles/charges can be significant. As a result dipole moments associated with the LC material may tend to be normal to the interface to maximize their interaction (*7*). This effect is essentially *short range* and never goes beyond a few tens of angstroms but it could be a big contribution to the LC anchoring.

Long-range van der Waals potential

The van der Waals potential between LCs and an anisotropic medium has been reviewed by previous researchers. In two classic papers, Dubois-Violette and de Gennes (*8, 9*) have shown that the more polarisable axis of a LC will align parallel to the more polarisable directions of the surface and the angular dependence can be separated out in the potential by using a simple expression:

$$U = U_0 \sin^2 \theta, \tag{1}$$

*Corresponding author. Email: pbos@lci.kent.edu

ISSN 0267-8292 print/ISSN 1366-5855 online

DOI: 10.1080/02678290801939244
http://www.informaworld.com

where U_0 denotes the van der Waals potential with LC aligned in its preferred direction and θ is the angle between the two more-polarisable axes. Many other researchers have followed the same $\sin^2\theta$ model (*10, 11*) or $P_2(\cos\theta)$ model (*12, 13*).

More recently, Lu *et al.* (*14*), Vithana *et al.* (*15*) and Kang *et al.* (*16*) have shown that a LC with a positive dielectric anisotropy ($\Delta\varepsilon$) prefers parallel alignment (also called planar) on SiO_x, whereas a LC with a negative $\Delta\varepsilon$ prefers perpendicular alignment (also called homeotropic). Lu *et al.* (*14*) have explained the effect by considering the difference in van der Waals potential between parallel and perpendicular states, caused by the dielectric anisotropy of the LC.

Competition between long-range and short-range forces

Dubois-Violette and de Gennes (*9*) discussed the so-called local Fredericks transitions. A solid/nematic interface was considered, where long-range van der Waals torques favour perpendicular alignment, whereas short-range effects tend to induce a parallel alignment. The final orientation depends on their relative strength. The authors proposed using the following equation to express the total energy:

$$2F = -\int_{\delta}^{\infty} u(z)\sin^2\theta\,\mathrm{d}z + 2\int_{\delta}^{\infty} K\left(\frac{\mathrm{d}\theta}{\mathrm{d}z}\right)^2 \mathrm{d}z + 2W\sin^2\theta_0. \quad (2)$$

As shown in Figure 1, z is the distance from surface, δ is an infinitesimal isotropic gap to prevent the energy from diverging, θ_0 is the angle that the director deviates from the short-range torque preferred direction (surface normal) on the interface and θ is the actual anchoring angle. F is the total free energy, $u(z)$ is the van der Waals potential, K is the elastic constant of the LC and W is the surface anchoring energy that corresponds to short-range interactions.

Two anchoring transitions were predicted: parallel $\leftrightarrow$ conical (tilted) and conical $\leftrightarrow$ perpendicular. These anchoring transitions are called *local Fredericks transitions* because they are caused by local (short-range) forces. Blonov and Sonnin (*17, 18*) have successfully demonstrated local Fredericks transitions on mica cleavages covered by an amorphous film.

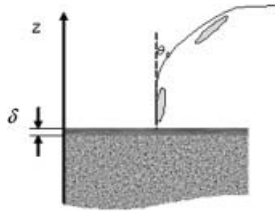

Figure 1. Illustration of the Dubois-Violette and de Gennes model.

Topography

Topography is also an important factor in LC alignment. A classic view describes the surface of SiO_x as porous columns or periodic structures. LC molecules are believed to align parallel to the surface everywhere and the orientation of director is determined when the elastic distortion energy is minimized (*19–22*). A more recent study by Papanek and Martinot-Lagarde (*23*) has shown that other factors such as order electricity are important in the case of porous SiO_x surface.

However, studies have shown that the porous surface morphology exists only when evaporation angle (the angle between the SiO_x beam and substrate surface) is small. Evaporation at a medium or larger angle (e.g. $>30^\circ$) results in compact structure and smooth surface (*24, 25*). We have confirmed this using atomic force microscopy (AFM). In this paper, we restrict our attention to the particular case of large-angle deposited SiO_x (LAD-SiO_x), where topography is unlikely to have a significant effect on the LC alignment. The fact that different LC materials may choose completely different orientation on the same SiO_x substrate also indicates a mechanism that cannot be explained by the elastic distortions of director.

Scope of this paper

In this paper we report an experimental observation of anchoring transitions on LAD-SiO_x that we believe to result from the change of the relative strength of long-range and short-range contributions. Further, we will present our study on the topography of LAD- SiO_x, and a comparison between thermally evaporated LAD- SiO_x and e-beam evaporated quartz. We also report thermally induced anchoring transitions and the effect of temperature on anchoring transitions. A thermal desorption study of LC components on SiO_x provided us with information about the short-range interactions. Related to the long-range force, we observed that SiO_x thickness has the ability to shift the anchoring, even if it is screened by another thin film. Also, we propose a model to describe the LC anchoring on SiO_x and use this model to explain our experimental results.

2. Theory

Our ideas are based on the model proposed by de Gennes and Dubois-Violette (*9*). The theory is related to anchoring transitions that are seen on smooth SiO_x (such as the surface of LAD-SiO_x in our case), and is made with three assumptions that have previously been accepted by many others as discussed in the last section:

(1) Short-range dipolar interactions tend to align dipole moments perpendicular to the SiO_x surface.
(2) Long-range van der Waals interaction tends to align the more polarisable directions of LC along with those of the alignment layer.
(3) We can neglect surface topography and resulting steric forces for the case of large angle SiO_x alignment layers used in this study.

From the first assumption it follows that for a LC with a positive $\Delta\varepsilon$ (the dipole is more or less along the long molecular axis) a perpendicular boundary condition is preferred by short-range dipolar interactions. For a LC with a negative $\Delta\varepsilon$ a parallel boundary condition is preferred because the dipole is more or less perpendicular to the long molecular axis.

The second assumption gives the long-range force preference of bulk LC orientation as a function of dielectric anisotropy. We assume that SiO_x is more polarisable in the plane of the film than perpendicular to it. This assumption is consistent with the molecular structure of SiO_x thin films. According to Philipp (*26, 27*) and Hohl *et al.* (*28*) the molecular structure of SiO_x can be described in a random binding model. In the model every silicon atom is combined with four other atoms (either oxygen or another silicon) to form a matrix. Considering the dimension of this matrix, electrons should find it easier to move in-plane than out-of-plane. Therefore LAD-SiO_x should be more polarisable in the surface plane than along its normal direction.

As a result a LC with a positive $\Delta\varepsilon$ tends to align parallel to the surface but a LC with a negative $\Delta\varepsilon$ tends to align perpendicular to the surface. In both cases the electrically more polarisable directions of the LC is parallel to the more polarisable directions of SiO_x.

The third assumption holds true in our particular case of large-angle deposited SiO_x, where we have found that elastic distortion energy caused by the surface topography is one order of magnitude smaller than the measured anchoring energy. This allows us to neglect the elastic energy distortion on SiO_x surfaces.

Table 1. The preference in LC orientation for long-range/short-range torques.

LC dielectric anisotropy	Long-range van der Waals force preferred LC orientation	Short-range dipolar force preferred LC orientation
Positive	Parallel to the interface	Perpendicular to the interface
Negative	Perpendicular to the interface	Parallel to the interface

Based on the above assumptions we can list the orientational preferences of both the long-range van der Waals force and short-range dipolar forces in Table 1. A schematic illustration is also shown in Figure 2. It is clear that long-range van der Waals force and short-range dipolar forces have opposite preference in LC orientation direction. The final LC anchoring on SiO_x is determined by the competition between the long-range van der Waals force and short-range surface dipolar forces.

This hypothesis may explain many effects that were found hard to explain before. For example, it has been found that the orientation of the first layer of LC can differ appreciably from the orientation in the bulk. Reznikov *et al.* (*29*) reported that the first layer (or a monolayer) of 5CB aligns perpendicularly at the LC/quartz surface, but the bulk of 5CB shows parallel anchoring. A similar phenomenon has been reported on different substrates like polymers, crystals and glass (*30, 31*).

Following the model that Dubois-Violette and de Gennes proposed (*9*) we start with equation (2) to described the free energy in the situation where long-range van der Waals torque prefers parallel alignment whereas short-range torques prefer perpendicular alignment.

We limit the consideration to either planar or perpendicular alignment ($\theta_0=\theta$) so that the more

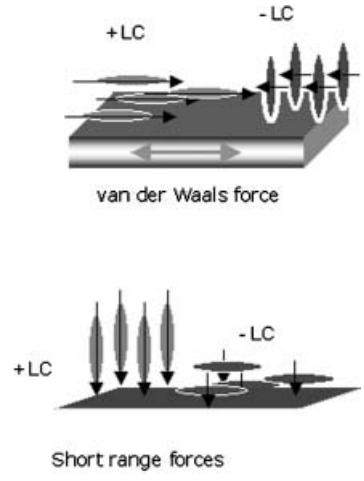

Figure 2. The preference in LC orientation for long-range/short-range forces.

complicated conical situation can be excluded. We further assume that there is no deformation of LC director orientation, so we can neglect the elastic energy term in the free energy. This assumption may not be completely true but it should give us a fairly good approximation since the short-range interaction only works on the first layer of LCs. Therefore the formula is simplified to:

$$2F = -\int_{\delta}^{\infty} u(z)\sin^2\theta\,\mathrm{d}z + W\sin^2\theta. \tag{3}$$

Let us define $U = \int_{\delta}^{\infty} u(z)\mathrm{d}z$ then

$$2F = -U\sin^2\theta + W\sin^2\theta, \tag{4}$$

where θ can only be 0 (perpendicular) or $\pi/2$ (parallel) from the surface normal.

Let us use superscript + and − to denote the material with positive and negative dielectric anisotropy, respectively. Now let us consider the following situations

A LC with a positive $\Delta\varepsilon$.

When $\theta=0$, $F^{+}=0$; when $\theta=\pi/2$, $2F^{+}=W^{+}-U^{+}$.

So, when $W^{+}<U^{+}$, the system has lower energy in parallel state and when $W^{+}>U^{+}$ perpendicular alignment gives lower energy.

A LC with a negative $\Delta\varepsilon$.

Similar to Equation (4), for a LC that has a negative $\Delta\varepsilon$ the total energy can be written as

$$2F^{-} = -U^{-}\cos^2\theta + W^{-}\cos^2\theta \tag{5}$$

to reflect the preference of long range and short range torque.

When $\theta=0$, $2F^{-}=W^{-}-U^{-}$; when $\theta=\pi/2$, $F^{-}=0$.

So, if the short-range interaction is strong enough, i.e. $W^{-}>U^{-}$, a planar anchoring is preferred. On the other hand, if $W^{-}<U^{-}$and van der Waals wins, a perpendicular alignment is preferred.

A mixture containing both negative and positive $\Delta\varepsilon$ *LCs.*

In a mixture that contains LCs with both positive and negative $\Delta\varepsilon$ we have to take into consideration of the distribution of each component in the bulk and on the surface. A simplified model would be two active components (one positive and one negative) in a neutral base. Here, we use x to denote the concentration of one component in the mixture:

$$x^{+} = m^{+}/\left(m^{+}+m^{-}+m^{neutral}\right), \tag{6}$$

$$x^{-} = m^{-}/\left(m^{+}+m^{-}+m^{neutral}\right), \tag{7}$$

where m is the amount of the component in the mixture.

For any component, it is safe to assume that the bulk concentration in the cell is the same as x. However, the surface concentration can deviate from x appreciably. The surface concentration of a component can be represented by its surface coverage ratio, Θ, defined as

$$\Theta^{+} = n^{+}/N^{+}, \tag{8}$$

$$\Theta^{-} = n^{-}/N^{-}, \tag{9}$$

where n is the number of adsorbed molecules and N is the maximum number of this component molecules that can be adsorbed, i.e. the total available sites for this particular component. As can be seen we have assumed that the total available sites could be different for different component because of their very different properties.

Therefore, the total energy can be expressed as

$$\begin{aligned} 2F = &-x^{-}U^{-}\cos^2\theta + \Theta^{-}W^{-}\cos^2\theta \\ &-x^{+}U^{+}\sin^2\theta + \Theta^{+}W^{+}\sin^2\theta. \end{aligned} \tag{10}$$

The difference in energy between perpendicular alignment and parallel alignment is

$$\begin{aligned} 2\Delta F = 2[F(0)-F(\pi/2)] = \\ -x^{-}U^{-} + \Theta^{-}W^{-} + x^{+}U^{+} - \Theta^{+}W^{+}. \end{aligned} \tag{11}$$

An anchoring transition takes place at the critical point when $\Delta F=0$, i.e.

$$x^{-}U^{-} - \Theta^{-}W^{-} = x^{+}U^{+} - \Theta^{+}W^{+}. \tag{12}$$

3. Experiments and results

General experimental processes

SiO_x alignment layer.

Two types of silicon oxide films were used: thermally evaporated SiO_x and e-beam evaporated SiO_2. In this paper, they are referred to simply as SiO_x and SiO_2.

In most of the experiments, SiO_x thin films were used. They were prepared by thermally evaporating silicon monoxide (SiO) powders onto substrates at a

large angle of incidence. The thickness of coating is measured in-situ by an oscillating quartz crystal thickness monitor. The reading of the thickness monitor has been calibrated with ellipsometry measurement data. The deposition rate was controlled to be 2~3 Å s^{-1}. Residual pressure was controlled to be within 5×10^{-6} to 2×10^{-5} torr implemented by back-bleeding through a needle valve.

E-beam evaporated SiO_2 thin films were used only to compare with SiO_x and is especially denoted where it is used. The films were prepared by evaporating quartz pellets by e-beam using the same process parameter as used for thermal evaporation. The e-beam evaporator we used is of the same basic geometry as the thermal evaporator, and should produce substrates for a fair comparison.

Cell construction.

Substrates coated with SiO_x or SiO_2 were assembled into sandwich cells with anti-parallel evaporation directions on two plates. The cell gap used in the experiments was ~20 µm unless otherwise stated. A larger cell gap enabled us to achieve better accuracy in pretilt measurement using crystal rotation method. However, we have found our results also reproducible on other cell gaps, e.g. 1.0 µm, 4 µm and 10 µm. Cells were filled in vacuum by capillary force at room temperature.

General examination methods and pretilt measurement.

Filled cells were examined on a light table between two crossed polarisers. Cells with perpendicularly aligned LC should always look dark when rotated. But for cells with parallel LC orientation, bright-dark alternation will be observed when rotated. Pretilt angles of liquid crystal were measured by three methods: conoscopy (*32*), crystal rotation (*33*) and optical retardation method. The first two methods have relatively high accuracy and their relative error has been found to be within 0.5°. All of the pretilt data except that in the *screening effect* (see section below) was obtained using conoscopy and crystal rotation methods. In the *screening effect* experiments pretilt angles were calculated from optical retardation data measured using a tuneable compensator. The optical retardation can be expressed as

$$\gamma = \Delta n d = (n_{eff} - n_o) d, \tag{13}$$

where the effective extraordinary refractive index of the LC satisfies

$$n_{eff} = n_e n_o \Big/ \sqrt{n_e^2 \cos^2\theta + n_o^2 \sin^2\theta} \tag{14}$$

and θ is the pretilt angle from the surface normal. From equations (8) and (9) we get

$$\theta = \arcsin\left[\sqrt{\left(n_e^2 - n_e^2 n_o^2 \Big/ (\gamma/d + n_o)^2\right) \Big/ \left(n_e^2 - n_o^2\right)}\right]. \tag{15}$$

The refractive index n_e, n_o and cell gap, d, were measured in separate experiments.

Physicochemical properties of SiO_x

Stoichiometry.

The stoichiometry of SiO_x/SiO_2 thin films was studied by X-ray photoelectron spectroscopy (XPS). The spectra in Figure 3 show that e-beam evaporated SiO_2 always has the atomic ratio of O/Si very close to 2/1. But for thermally evaporated SiO_x we have seen the ratios from 1.2 to 1.7, which implies an oxygen deficient chemical structure. Analysis of the Si 2*p* peak in Figure 4 shows that e-beam evaporated SiO_2 has a major contribution from SiO_2 and a tiny one from SiO. On another hand, the Si 2*p* peak for thermally evaporated SiO_x shows contributions from SiO_2, SiO and a small part of silicon. Angular resolved measurements allow us to see the structure of SiO_x as a function of distance from the surface. The results show that the surface stoichiometry does not deviate much from the bulk of the SiO_x film.

Surface topography.

Surface topography of obliquely evaporated SiO_x was examined by AFM. Figure 5 shows a typical AFM images of SiO_x surfaces measured by different scanning modes. The cross-section analysis (Figure 5 (d)) of the sample shows that the topographic features are usually around 5 nm in height but 200 nm in width (note that the horizontal and vertical scaling in the figures is very different). The measured RMS roughness is generally less than 0.7 nm. We have calculated the elastic distortion energy of LC induced by SiO_x surface roughness, based on AFM data. The results show that maximum anchoring energy could be possibly achieved is about one order of magnitude smaller than the experimentally measured anchoring energy.

We also studied the evolution of surface topography with the increase of SiO_x layer thickness. The results in Figure 6 show little changes in either surface roughness or its anisotropy, defined as the difference in RMS roughness when sample is scanned along evaporation direction and perpendicular to evaporation direction, when the thickness increases from ~30 nm to ~350 nm.

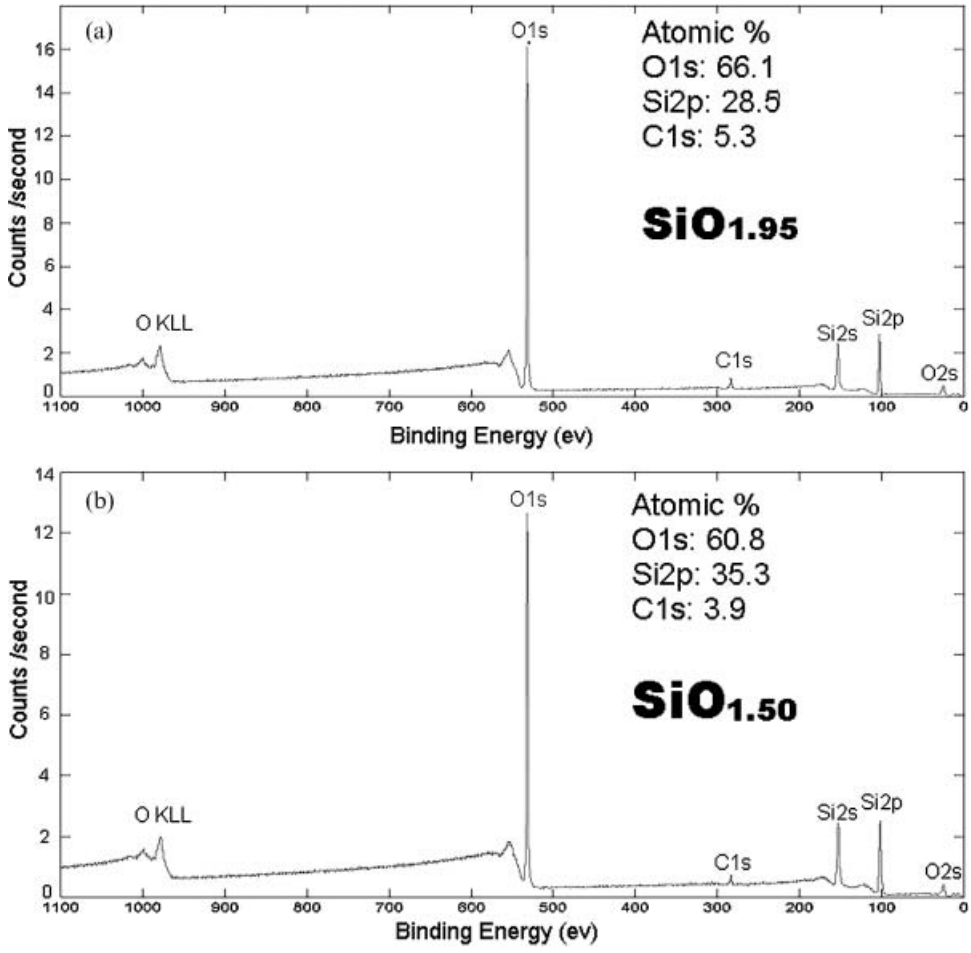

Figure 3. XPS spectrum of thermally evaporated SiO_x and e-beam evaporated SiO_2 measured with a 45° takeoff angle.

Anchoring transitions on LAD-SiO_x thin films

Change in LC mixture composition.

To study the effect of a large longitudinal dipole, a commercial LC mixture from Merck (hereafter referred as LC1, $\Delta\varepsilon=-5.7$, $\Delta n=0.164$) was filled into SiO_x cells. LC1 has a large negative dielectric anisotropy. It assumes parallel anchoring on SiO_x. Another commercial single component LC, known as 5CB or K15 (4-cyano-4′-*n*-pentylbiphenyl) was filled into identical cells and found to assume parallel anchoring as well. The molecule of 5CB has a cyano group at the end of its long axis, thus a big longitudinal dipole. We added 5CB into LC1 and filled the mixtures into LAD-SiO_x cells. At room temperature, when the concentration of 5CB in the mixture is less than 3% (by weight, the same in the following) the mixture chooses parallel anchoring. When the concentration of 5CB is greater than ~3% an anchoring transition takes place so that the mixture has perpendicular alignment. Increasing the concentration of 5CB to ~55% another transition happens so that the alignment is parallel again. Figure 7 shows the tilt angle of LC director (with respect to substrate surface) as a function of 5CB concentration. As mentioned in the introduction, Wen *et al.* (*4*) observed similar effect when mixing a liquid crystal that has a large negative $\Delta\varepsilon$ with other materials that has longitudinal cyano-like groups.

To study the effect of a large lateral dipole, 1-ethoxy-4-(4′-*trans*-propylcyclohexylcarboxy)-2,3-dicyanobenzene (hereafter referred to as C3), a chemical that has large negative $\Delta\varepsilon$, was used. Materials with a similar structure to C3 are used as dopants in making commercial LCs with negative $\Delta\varepsilon$. One commercial LC from Merck (hereafter referred as LC2, $\Delta\varepsilon=-2.7$, $\Delta n=0.164$) was mixed with C3 and filled into LAD-SiO_x cells. The reason we chose LC2 is that C3 has a good solubility in it and anchoring transitions can be more clearly demonstrated. LC2 by itself chooses perpendicular orientation on SiO_x. We were not able to know how C3 aligns on SiO_x because it does not exhibit a nematic phase by itself. We added increasing amounts of C3 into LC2 and filled the mixtures into SiO_x cells. When the concentration

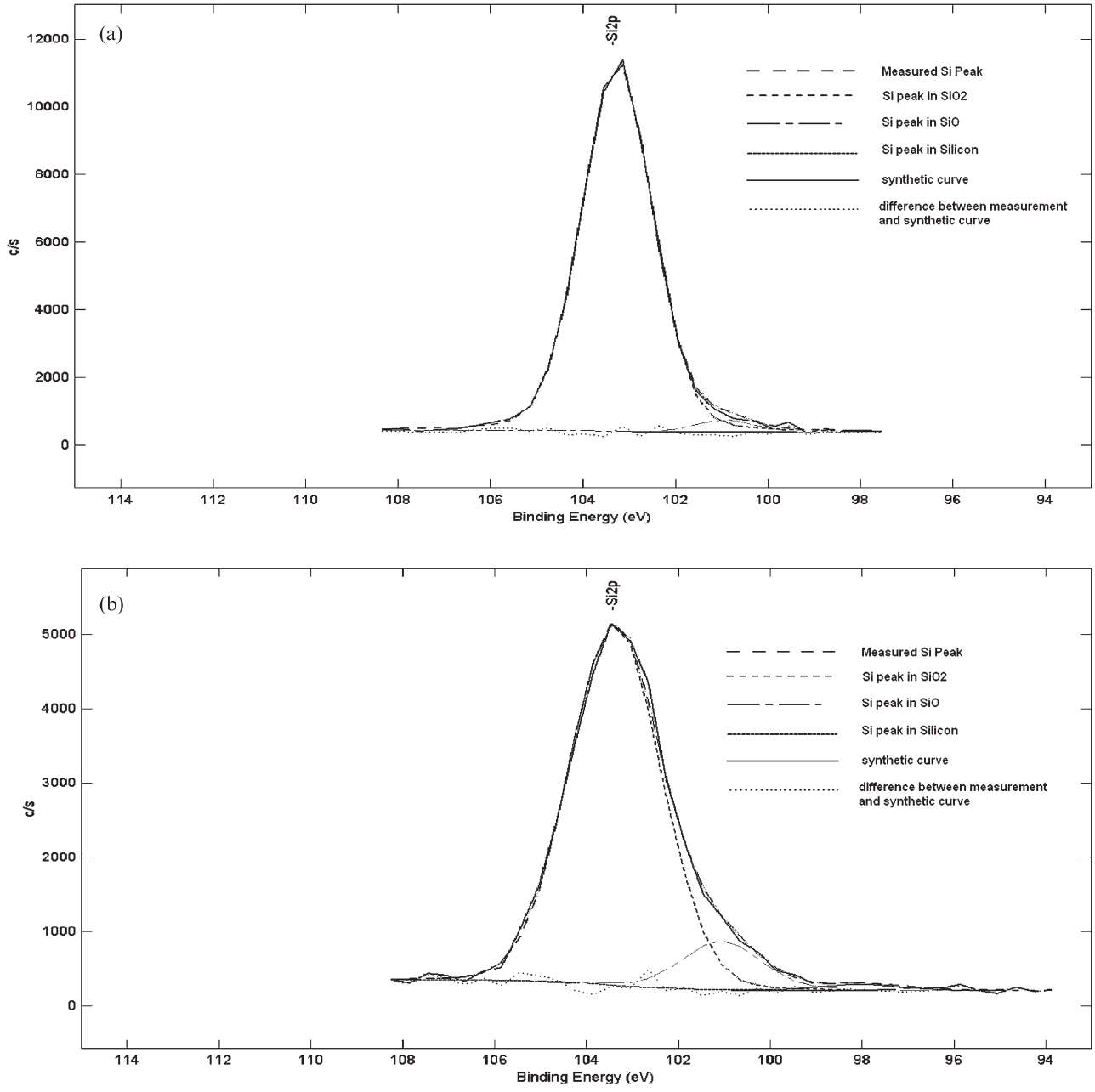

Figure 4. XPS spectrum analysis of silicon (Si 2*p*) in e-beam evaporated SiO_2 (a) and thermally evaporated SiO_x (b). Blue line is the characteristic peak of Si in SiO_2; cyanic line is the characteristic peak of Si in SiO; magenta line is the characteristic peak of Si in Si crystal; black line is the measured Si peak; red line is the synthetic peak based on characteristic Si peak in SiO_2, SiO and Si crystal.

of C3 is equal to or less than 5% the mixture still aligns perpendicularly. However, starting from 6% an transition takes place and finally changes the LC anchoring into parallel when the concentration of C3 is equal to or larger than 8%, as can be seen in Figure 8(a).

Another observation is that the alignment can also be swung back to perpendicular with the addition of small amount of 5CB to the mixture composed of LC2 and more than 8% of C3. Figure 8(b) shows the transitions. Also seen from the plot is for mixtures with higher concentration of C3, larger amount of 5CB is needed to trigger the transition.

Temperature dependence of the anchoring transition.

We made a mixture composed of 1/3 LC1 and 2/3 LC2. This mixture was filled into LAD-SiO_x cells and found to assume perpendicular alignment on SiO_x at

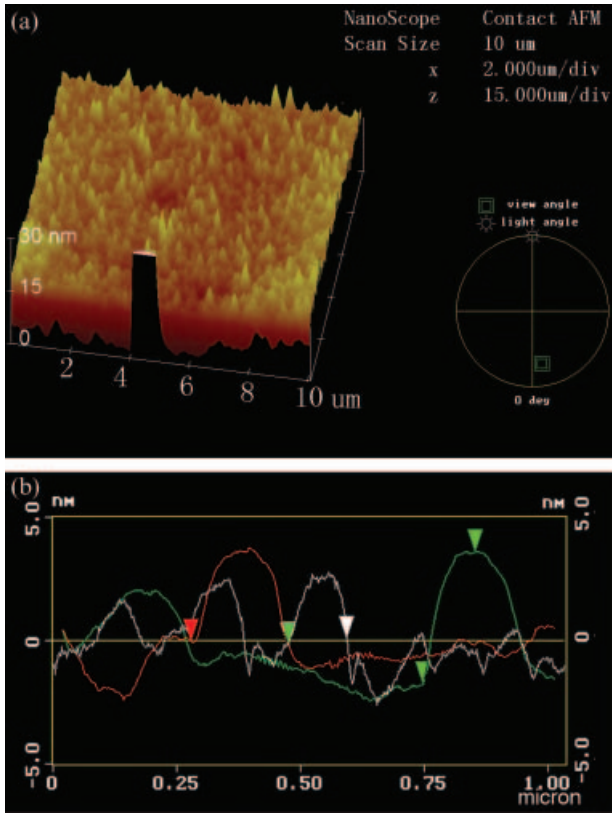

Figure 5. AFM image of SiO_x thermally evaporated at a medium angle: (a) 10 μm × 10 μm tapping mode 3D image; (b) 5 μm × 5 μm tapping mode 3D image; (c) 3 μm × 3 μm contact mode 2D image of friction; (d) cross-section analysis.

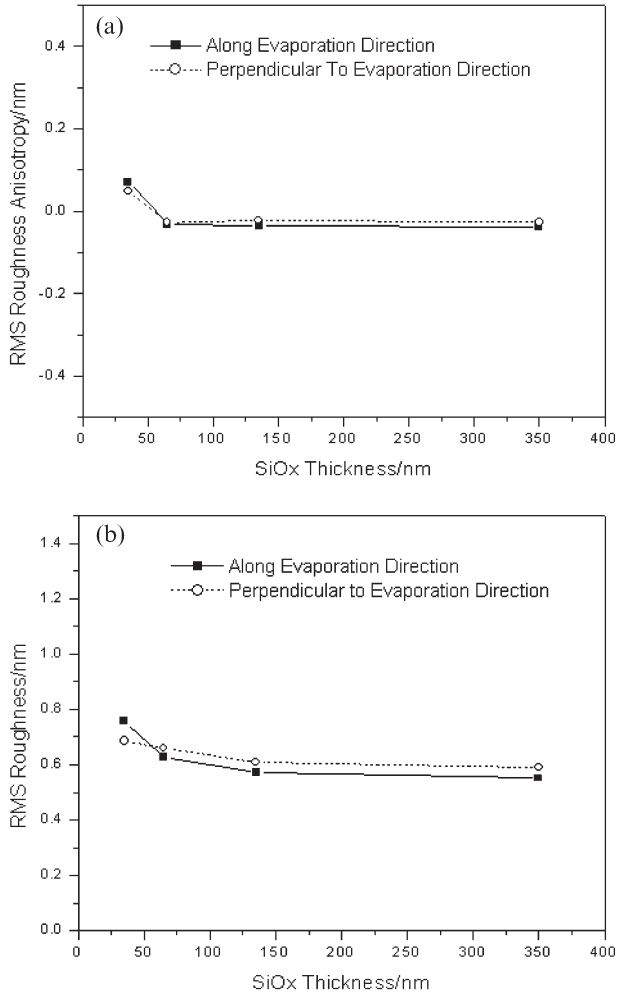

Figure 6. (a) RMS roughness of SiO_x surface as a function of layer thickness. (b) Anisotropy in surface roughness as a function of layer thickness.

room temperature. Cells were placed between two crossed polarisers with the evaporation direction 45° with the polariser axis. A He–Ne laser passes the polarisers and the sample along in the normal direction. We measured the transmitted light intensity as a function of temperature. We found that when the cell was heated the intensity of transmitted light increased. This effect becomes more abrupt when the temperature is beyond ~50°C. This phenomenon indicates that the optical retardation of the cell increases with the temperature, meaning a deviation of LC director from perpendicular to parallel orientation. Figure 9 shows the measured results for several mixtures. As can be seen the temperature dependence is different for different LC materials.

In the anchoring transitions described above (Figure 7) we observed a shift of anchoring transition point due to this temperature dependence effect. As shown in Figure 10, the first anchoring transition (at the lower concentration of 5CB) is obviously shifted due to the temperature change. The concentration of 5CB required to obtain perpendicular anchoring

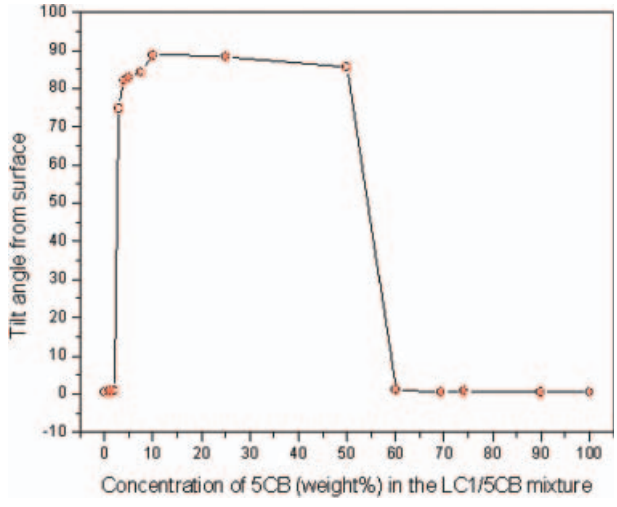

Figure 7. Anchoring transitions of LC mixtures (5CB/LC1) on SiO_x due to the change of the ratio of two components.

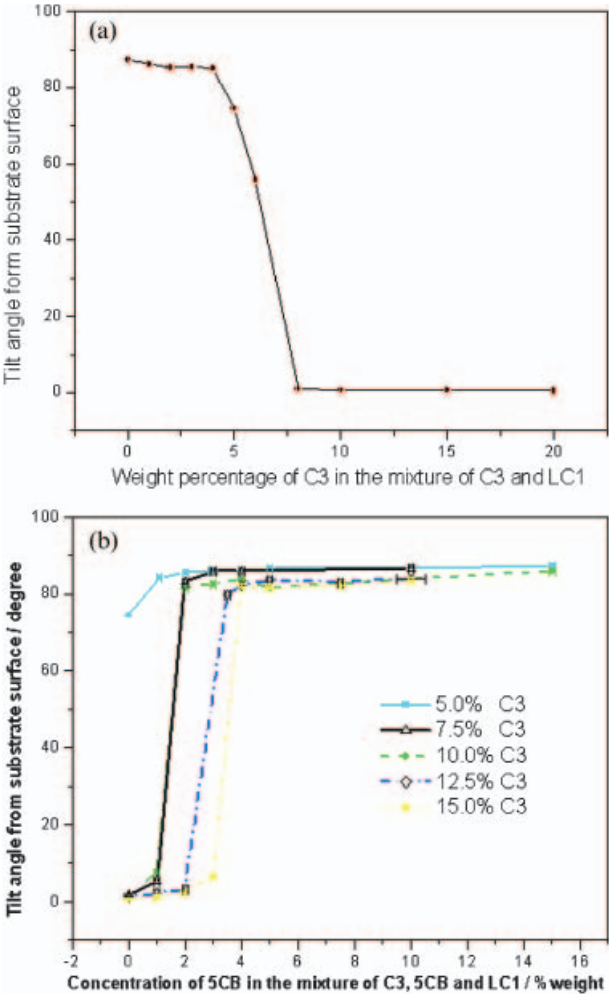

Figure 8. (a) The addition of material that has strong lateral dipole (C3) into LC2 leads to an anchoring transition from perpendicular to parallel; (b) the addition of a material with a strong longitudinal dipole (5CB) into the mixture of C3 and LC2 causes an anchoring transition from parallel to perpendicular.

(defined as the critical concentration) ascends when the temperature increases.

As can be also seen in Figure 10, we observed no temperature dependence on the second anchoring transition (that occurs at the higher concentration of 5CB). One reason is that since 5CB has a nematic–isotropic transition temperature as low as ~37°C the clearing point of the mixtures decreases when 5CB concentration increases, so we were unable to measure the anchoring transition point of mixtures with a high concentration of 5CB. However, judging from the available data we do not see any indication of noticeable thermal induced anchoring shift for the second transition.

To understand the temperature dependence of anchoring transition we studied the surface absorption of LCs on LAD-SiO_x by thermal desorption

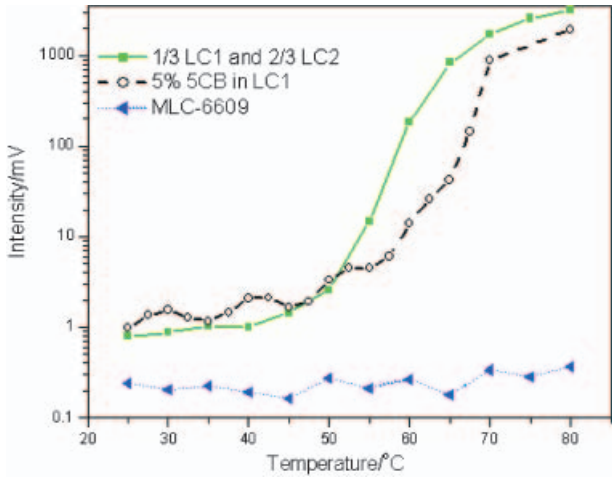

Figure 9. Intensity of transmitted light as a function of temperature. Samples were held between crossed polarisers with evaporation direction 45° with the polarizer axis. All cells have the same cell gap ~20 µm.

mass spectroscopy (TDMS). The results can provide information on the surface binding energy between LC molecules and SiO_x. Experiments were done on a Thermo Electron Polaris Q GCMS with a direct exposure probe (DEP). SiO_x was deposited onto both sides of aluminium foils and soaked into diluted C3 and 5CB solutions (0.3% by weight in isopropyl alcohol). After more than 8 h the foils were taken out and gently dried. Dried foils were cut into small pieces around 1 mm × 6 mm size to be compatible with the crucible in the DEP as well as to get good thermal conductivity thus accurate temperature on the samples. The crucible was then put into DEP and heated with a programmed temperature profile in vacuum. Desorbed materials were ionized and

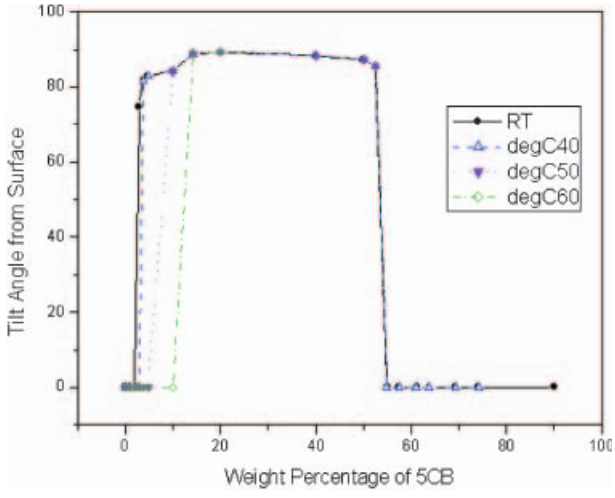

Figure 10. Temperature dependence of the anchoring transitions in a 5CB/LC1 mixture.

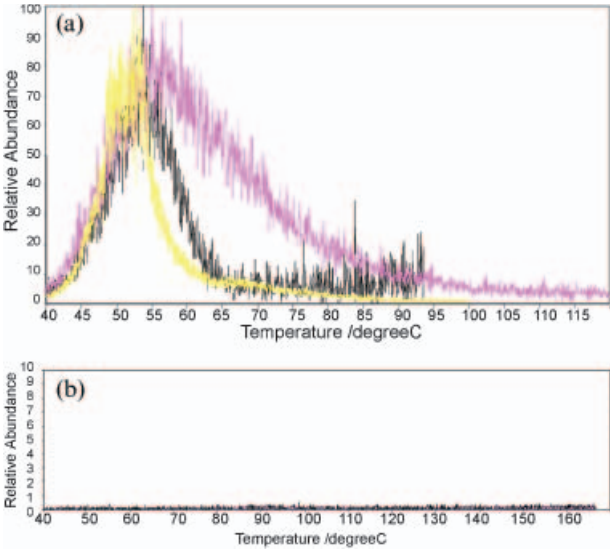

Figure 11. (a) Thermal desorption curve of 5CB; (b) thermal desorption curve of C3.

analysed by the mass spectrometer. Before the thermal desorption experiments we have already obtained the mass spectrum of 5CB and C3 so we can only look at 5CB and C3 spectral signatures. Figure 11(a) shows the desorption curve of 5CB measured from three different samples. As can be seen, the thermal desorption peak is at $55 \pm 2.5^{\circ}$C. The error probably comes from the difficulty in reproducing 5CB *monolayer* on each sample. We also tried to measure the thermal desorption curve of C3. Unfortunately, even if we increased the temperature to about 165°C we did not see any noticeable desorption of C3 on any sample, as shown in Fig. 11b. Considering the two lateral cyano groups on each C3 molecule and its relatively large molecular weight we conclude that C3 has a very strong surface interaction with SiO_x that prevents it from desorbing at a temperature lower than 165°C.

Dependence of anchoring transition on SiOx thickness.

We discovered that anchoring transitions depend on the thickness of the SiO_x layer. In our experiments SiO_x was thermally evaporated onto four identical glass substrates with identical deposition parameters but increasing layer thickness. Cells were made from these coated substrates and were filled with mixtures of LC1 and 5CB. As described above (Figure 7), we observed parallel-to-perpendicular and perpendicular-to-parallel anchoring transitions as the concentration of 5CB increases. But we also found that the anchoring transitions have different starting and ending points on SiO_x with different thickness. On the first transition where LC anchoring switch from

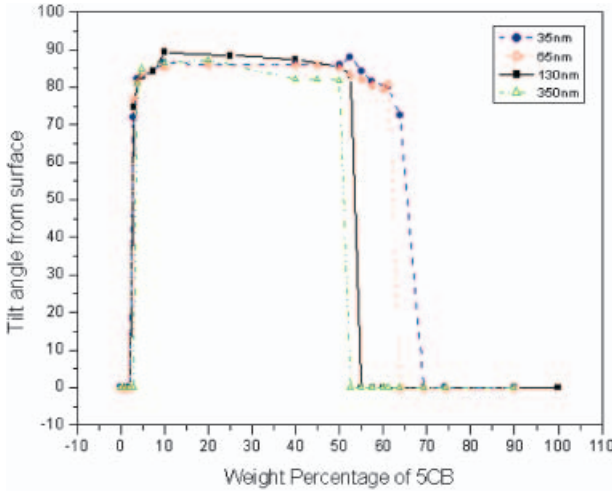

Figure 12. The anchoring transitions in a 5CB/LC1 mixture depend on the underlying SiO_x layer thickness.

planar to vertical (on the left in Figure 12) we did not notice any obvious change due to SiO_x thickness. However, on the second transition where LC anchoring switches from vertical to planar (on the right of Figure 12) we found that with a thicker SiO_x layer on the substrate, lower concentration of 5CB is needed to make the transition happen.

The SiO_x thickness dependence was observed even when the SiO_x layer was screened by other films. To show this effect we put a thin layer of polyimide (PI) on top of SiO_x. SE-7511L polyamic acid is widely used to produce PI alignment layers that give LC perpendicular anchoring.

In one experiment we fixed the top PI layer thickness and increased the SiO_x thickness from 0 to 130 nm. 5CB was filled into the cells. We found that the pretilt angle of 5CB (with respect to the surface) decreased when we increased the SiO_x thickness, even though SiO_x has been separated from 5CB by the PI layer. The results are shown in Figure 13(a).

In another experiment, PI 7511 layers with different thickness were coated onto substrates with fixed SiO_x thickness. 5CB was filled into the cell and tested for its alignment. The results show that 5CB forms perpendicular alignment when PI 7511 is thick enough. When the PI layer becomes thinner the pretilt decreases accordingly. At a certain point, the 5CB director jumps down and quickly changes into planar alignment. The experiment was repeated on bare ITO glass and ITO glass coated with 22 nm, 65 nm or 130 nm SiO_x. Similar results were observed, as shown in Figure 13(b).

Significantly, the same experiments using MLC-6609 (which has a negative $\Delta\varepsilon$) instead of 5CB produce no anchoring transition.

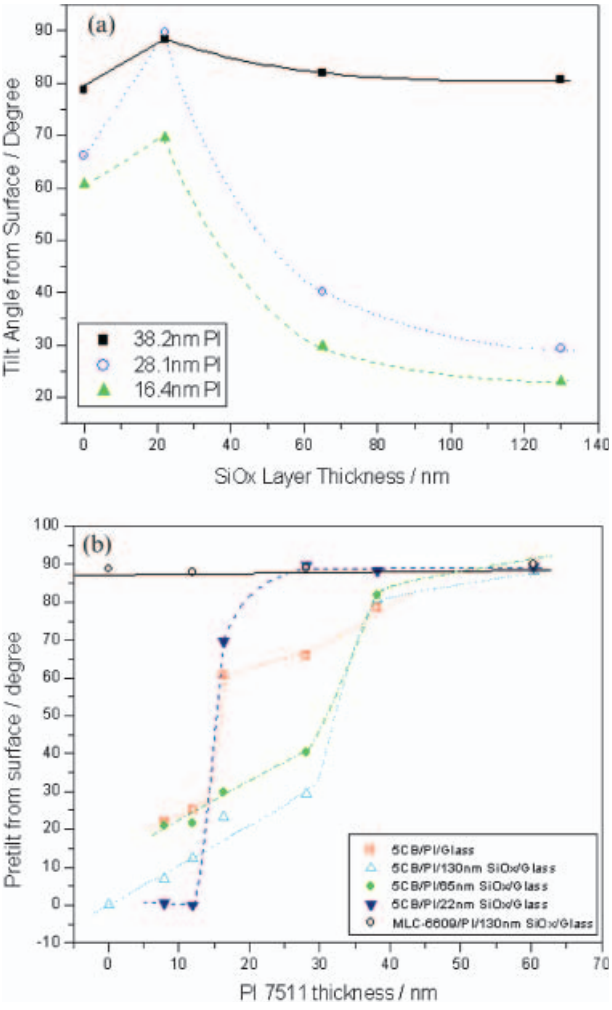

Figure 13. (a) The effect of SiO_x layer thickness on the alignment of 5CB screened by polyimide that prefers homeotropic anchoring. (b) Local Fredericks transitions induced by the screening effect of polyimide on top of SiO_x surface.

We also noticed that LC on the bare ITO glass (0 nm SiO_x) shows tilt angles very different from LC on other SiO_x substrates and does not fit into the transition curve in Figure 13(a). We believe that this is due to the very different surface wetting between glass and SiO_x. So the produced PI films are not directly comparable in thickness and other properties.

Alignment on SiO_2 vs. SiO_x.

Thermal and e-beam evaporation were used to produce two alignment layers, respectively, with identical thickness and process parameters. Cells were made and filled with LC1. As described above, LC1 assumes parallel anchoring on thermally evaporated SiO_x. However, it chooses perpendicular anchoring on e-beam evaporated SiO_2.

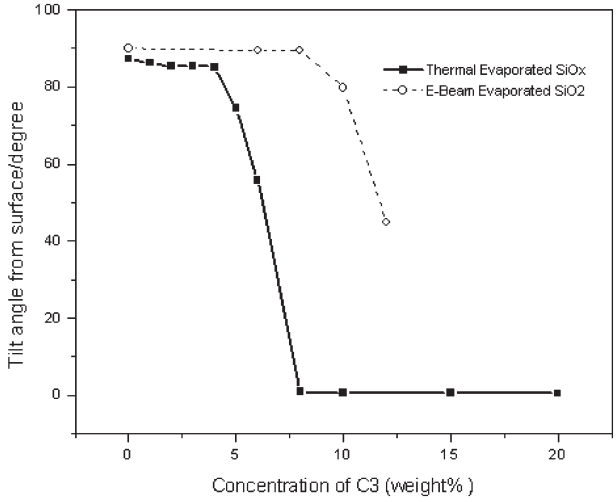

Figure 14. Comparison of the perpendicular-to-parallel anchoring transition of a C3/LC2 mixture on SiO_x and SiO_2 surfaces.

Further, we filled the mixture of LC2 and C3 into the SiO_2 cells. A perpendicular-to-parallel anchoring transition was observed similar to the one on SiO_x that we have shown in Figure 8(a). Nevertheless, we found that a significantly higher concentration of C3 was required before the anchoring transition could take place on SiO_2, compared to the result on SiO_x, as can be seen in Figure 14.

Summary of experimental results

Stoichiometry data shows that e-beam evaporated SiO_2 has a more saturated bonding structure compared to thermal evaporated SiO_x, which makes SiO_2 more stable and having less dangling bonds on the surface.

A liquid crystal with a positive $\Delta\varepsilon$ aligns parallel to LAD-SiO_x surface, whereas that with a moderate negative $\Delta\varepsilon$ aligns vertical to the SiO_x surface. However, a LC with a large negative $\Delta\varepsilon$ aligns parallel to the SiO_x surface.

The addition of small amount of a material that has a large longitudinal dipole to a LC that has a large negative $\Delta\varepsilon$ promotes vertical anchoring. However, a further increase in the amount of additive leads to parallel anchoring.

The addition of a material that has a large lateral dipole to a LC with a moderate $\Delta\varepsilon$ leads to an anchoring transition from vertical to parallel. Further introduction of small amount of material with a large longitudinal dipole can switch the anchoring back to vertical.

The critical concentration of additives that leads to anchoring transitions is highly depended on temperature. We expect this to be related to the absorption and thermal desorption on the SiO_x surface. Experimental data shows very different

thermal desorption temperature of two kinds of materials in our study.

SiO_x layer thickness has big influence on the critical concentration of the anchoring transition. The influence exists even if the SiO_x is separated from LC by another thin film.

E-beam evaporated SiO_2 has a better capability to generate vertical anchoring for LC with a large negative $\Delta\varepsilon$, compared to SiO_x.

The morphology of SiO_x films coated at a large angle shows little topography and is unlikely produce LC alignment by the principle of elastic energy minimization.

4. Discussions

Physicochemical properties of SiO_x and its influence on LC anchoring

The AFM study described above revealed that SiO_x thin films evaporated at a large angle exhibit densely packed structures. The surface roughness and anisotropy are so small that we believe surface topography and elastic distortion energy is unlikely to produce significant anchoring effects for the LC in our particular cases. It is also extremely hard to use topography to explain all the anchoring effects we observed in the experiments. A mechanism that has tighter relationship with the physical-chemical properties of SiO_x and LC molecules must therefore be considered.

Considering for the moment only Van der Waals forces, the liquid crystal will be expected to align with its more polarisable direction along with the more polarisable directions of the SiO_x. Therefore a LC with a positive $\Delta\varepsilon$ (longitudinal dipole) should prefer a parallel anchoring while a LC with a negative $\Delta\varepsilon$ (lateral dipole) should prefer a perpendicular anchoring

The stoichiometry of SiO_x also plays an important role in the liquid crystal anchoring. Un-occupied orbits or dangling bonds on the SiO_x surface tend to interact with the dipole moment strongly. So, a saturated surface will be more stable and less interactive to liquid crystal molecules compared to an unsaturated one. XPS data provide us with information on the surface of the SiO_x and SiO_2 thin films. We can see that on the thermally evaporated SiO_x surface silicon atoms are not saturated with oxygen, leaving many orbits accessible to LC dipoles. On the other hand, e-beam evaporated SiO_2 is more like a crystal structure with each Si bonded to four oxygens. As a result, we can expect a stronger short-range surface interaction between alignment layer and LC on SiO_x, compared to on SiO_2.

Anchoring transitions due to the change in LC mixture composition

The effect of the material that has a large longitudinal dipole.

It has been shown that the addition of small amount of 5CB into LC1 (which has a large negative $\Delta\varepsilon$) changes the anchoring on SiO_x from parallel to vertical. But, further increasing the amount of 5CB changes the anchoring back to parallel again. We have discussed the competition between long-range van der Waals force and short-range dipolar force in section 2. Here, we continue the discussion to explain the experimental data.

A LC mixture with a negative $\Delta\varepsilon$ is usually obtained by mixing a base LC with materials that have very high negative $\Delta\varepsilon$, such as C3. Since LC1 has a large negative $\Delta\varepsilon$ we expect it to contain a relatively large amount of negative additives. The effect of doing so on the alignment is twofold. On the one hand, an increased negative $\Delta\varepsilon$ will increase the anisotropy in van der Waals potential, making vertical alignment a more preferred LC anchoring on our substrates. On the other hand, the short-range interaction between SiO_x and negative additives such as C3 also will increase, but with parallel orientation as its more favourable anchoring direction. In the case of LC1 we believe that short-range dipolar interaction exceeds the long-range van der Waals interaction so that LC aligns parallel to SiO_x surface.

In contrast, 5CB is a small molecule with a large longitudinal dipole moment and a positive $\Delta\varepsilon$. It favours parallel anchoring by van der Waals force but vertical anchoring by short-range dipolar forces. When a small amount of 5CB is added to LC1 5CB molecules may bind with SiO_x surface preferentially, which substantially changes the anchoring preference of short range forces towards favouring homeotropic alignment. Due to the limited amount of 5CB in the mixtures being considered here, the bulk properties are unlikely to be noticeably altered so the long range force still favours homeotropic anchoring. Hence, both long range and short range interactions agree on the anchoring direction homeotropic alignment is obtained. Further increasing the amount of 5CB makes the $\Delta\varepsilon$ of bulk LC more positive and turns the van der Waals potential preference towards parallel anchoring. However, since the SiO_x surface becomes more or less saturated with 5CB molecules the short-range interaction does not increase. As a result, the long-range van der Waals force eventually exceeds and the LC changes back to parallel anchoring.

The effect of the material that has a large lateral dipole. In the experiment described above, C3 was mixed with LC2 causing an anchoring transition from vertical to parallel. Adding 5CB into the mixture shifts the anchoring back towards vertical. This effect can also be explained by our theory.

C3 has a two cyano groups hence a very large dipole moment perpendicular to its molecular long axis. The addition of C3 into LC2 leads to the increase of short range dipolar interaction between the mixture and SiO_x. It also contributes to the van der Waals potential due to its negative $\Delta\varepsilon$. But the increase in short range interactions must be more profound to cause the anchoring transition towards parallel.

The effect of adding 5CB afterwards is the same as discussed above. The reason why critical concentration of 5CB is quasi-proportional to the concentration of C3 lies in the short-range forces. For C3, the short-range force prefers parallel anchoring, whereas for 5CB it prefers vertical anchoring. The result is that more 5CB is needed in a system containing more C3 to make the overall surface short-range interaction also prefer perpendicular alignment.

Temperature dependence of anchoring transition

We have reported the temperature dependence of LC anchoring on LAD-SiO_x. Previous discussions (*34–36*) on similar topics have proposed use of the temperature dependence of the order parameter (S) to explain the effect. Although this theory has been successful in many aspects, we propose another possible explanation that we found to be useful in discussing the particular phenomenon we observed in our experiments.

Normally the surface absorption of a material can be described by the *surface coverage ratio* Θ, which satisfies the following equation (*37*):

$$\Theta = \frac{Ax\exp(-\Delta H/k_BT)}{1+Ax\exp(-\Delta H/k_BT)}, \tag{16}$$

where A is a constant, x is the concentration of adsorbent, ΔH is the enthalpy of the adsorption process, k_B is the Boltzman constant and T is temperature.

Letting

$$\Delta H = -k_BT^0, \tag{17}$$

where T^0 is the *characteristic temperature* of the thermal desorption process,

$$\Theta = \frac{Ax\exp(T^0/T)}{1+Ax\exp(T^0/T)}. \tag{18}$$

We know from the thermal desorption data (Figure 11) that the characteristic temperature is ~55°C for 5CB on SiO_x but higher than 165°C for C3.

Now consider the example of 5CB in LC1. The *surface coverage ratio* of 5CB is

$$\Theta_{5CB} = \frac{A'x_{5CB}\exp(T^0_{5CB}/T)}{1+A'x_{5CB}\exp(T^0_{5CB}/T)}. \tag{19}$$

Suppose the original concentration of C3-like material in LC1 is x^0_{C3}, its concentration in the mixture should be $x_{C3}=x^0_{C3}(1-x_{5CB})$. The *surface coverage ratio* of C3 is therefore

$$\Theta_{C3} = \frac{A''x^0_{C3}(1-x_{5CB})\exp(T^0_{C3}/T)}{1+A''x^0_{C3}(1-x_{5CB})\exp(T^0_{C3}/T)}. \tag{20}$$

At the critical point where an anchoring transition occurs,

$$\begin{aligned} &x^0_{C3}(1-x^{critical}_{5CB})U_{C3} - \frac{A''x^0_{C3}(1-x^{critical}_{5CB})\exp(T^0_{C3}/T)}{1+A''x^0_{C3}(1-x^{critical}_{5CB})\exp(T^0_{C3}/T)}W_{C3} \\ &= x^{critical}_{5CB}U_{5CB} - \frac{A'x^{critical}_{5CB}\exp(T^0_{5CB}/T)}{1+A'x^{critical}_{5CB}\exp(T^0_{5CB}/T)}W_{5CB} \end{aligned} \tag{21}$$

When the concentration of 5CB is relatively small, the coverage ratio of 5CB should also be small. So,

$$\Theta_{5CB} = \frac{A'x_{5CB}\exp(T^0_{5CB}/T)}{1+A'x_{5CB}\exp(T^0_{5CB}/T)} \approx A'x_{5CB}\exp(T^0_{5CB}/T). \tag{22}$$

Since 5CB concentration is small the concentration of C3 will be about x^0_{C3}. Due to the relatively high thermal desorption temperature of C3 (>165°C), it is reasonable to assume that the surface coverage ratio is close to 1 and the change in surface coverage ratio of C3 due to temperature or 5CB concentration is negligible.

So the critical point relies on:

$$\begin{aligned} &x^{critical}_{5CB}U_{5CB} - A'x^{critical}_{5CB}\exp(T^0_{5CB}/T)W_{5CB} = \\ &x^0_{C3}U_{C3} - \Theta^0_{C3}W_{C3} = C(\text{constant}), \end{aligned} \tag{23}$$

$$x^{critical}_{5CB} = C/\left(U_{5CB} - A'W_{5CB}\exp(T^0_{5CB}/T)\right). \tag{24}$$

Since C3 prefers parallel alignment by itself,

$$C = x^0_{C3}U_{C3} - \Theta^0_{C3}W_{C3} < 0. \tag{25}$$

Let

$$\alpha = -A'W_{5CB}/C, \quad \beta = -U_{5CB}/C, \tag{26}$$

$$x^{critical}_{5CB} = 1/\left[\alpha\exp(T^0_{5CB}/T) - \beta\right], \tag{27}$$

where α, $\beta>0$. Now let us consider the effect of temperature at anchoring transition point.

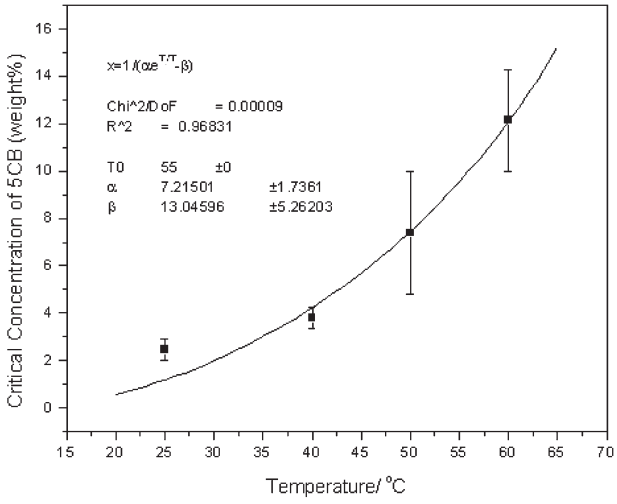

Figure 15. The critical concentration of 5CB in the planar-to-homeotropic anchoring transition of 5CB/LC1 mixtures as a function of temperature.

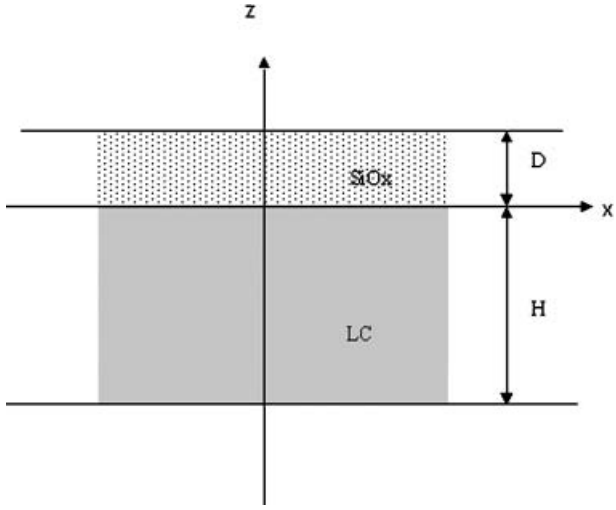

Figure 16. The cross-section of a half slab of a LC cell.

When T increases, $\alpha\exp\left(T_{5CB}^{0}/T\right)$ decreases and $1/\left[\alpha\exp\left(T_{5CB}^{0}/T\right)-\beta\right]$ increases. So as a result, the critical concentration of 5CB increases with temperature. Using equation (27) we were able to fit the critical concentration as a function of temperature in Figure 15. This explains the rising edge in Figure 10.

When the concentration of 5CB is large the absorption on SiO_x may be saturated even at relatively high temperature. Hence, there is no obvious temperature dependence on the falling edge in Figure 10.

Dependence of van der Waals potential on SiO_x layer thickness

The Effect of SiO_x thickness on anchoring transitions.

The van der Waals potential between two infinite flat surfaces is given by

$$W=-A/12\pi D^2. \tag{28}$$

de Gennes (*15, 16*) used this approach by assuming that there is an infinitesimal distance, δ, between the alignment layer and LC layer. However, to understand the anchoring transition dependence on SiO_x thickness this is inadequate. In this paper, we follow the method described by Israelachvilli (*38*) to deduct the influence of SiO_x thickness on van der Waals potential.

Let us start with the basic van der Waals interaction potential between two molecules:

$$w(r)=-\frac{C}{r^6} \tag{29}$$

Consider the half slab of a LC cell, as shown in Figure 16.

For molecules in a circular ring of cross-sectional area $dxdz$ and radius x, the ring volume is $2\pi xdxdz$. The number of molecules in the ring will be $2\pi\rho xdxdz$;

$$r=\sqrt{x^2+z^2}. \tag{30}$$

The net interaction for a LC molecule at a distance h from the SiO_x surface will therefore be

$$\begin{aligned} w(D) &= -2\pi C\rho\int_{z=h}^{z=h+D}\mathrm{d}z\int_{x=0}^{x=\infty}\frac{x\,\mathrm{d}x}{\sqrt{z^2+x^2}^6} \\ &= \frac{\pi C\rho}{2}\int_{z=h}^{z=h+D}\mathrm{d}z\frac{1}{\left(z^2+x^2\right)^2}\Big|_{x=0}^{x=\infty} \\ &= \frac{\pi C\rho}{2}\int_{z=h}^{z=h+D}\frac{\mathrm{d}z}{z^4}=-\frac{\pi C\rho}{6}\frac{1}{z^3}\Big|_{h}^{h+D} \\ &= -\frac{\pi C\rho}{6}\left[\frac{1}{h^3}-\frac{1}{(h+D)^3}\right]. \end{aligned} \tag{31}$$

To calculate the van der Waals potential between the LC and SiO_x layer per unit area, we need to integrate this over the thickness of LC layer. As de Geness pointed out, we have to assume an infinitesimal distance, δ, between the alignment layer and LC layer to prevent the integration from diverging. δ should be of the magnitude of absorbed monolayer thickness, a good estimation would be $\sim$1 nm.

Therefore, we have

$$w(D,H) = -\frac{\pi C\rho_1\rho_2}{6}\int_{h=\delta}^{h=H}\left[\frac{1}{h^3}-\frac{1}{(h+D)^3}\right]\mathrm{d}h$$
$$= -\frac{\pi C\rho_1\rho_2}{6}\left[-\frac{1}{2}\frac{1}{h^2}\Big|_{\delta}^{H}+\frac{1}{2}\frac{1}{(h+D)^2}\Big|_{\delta}^{H}\right] \quad (32)$$
$$= -\frac{\pi C\rho_1\rho_2}{12}\left[\frac{1}{(\delta+D)^2}-\frac{1}{(H+D)^2}-\frac{1}{\delta^2}+\frac{1}{H^2}\right].$$

In our experiments, H (half cell gap) is about 10 μm, D (SiO_x thickness) is from 0.035 μm to 0.35 μm and δ is about 0.001 μm. Therefore, $H \gg D \gg \delta$ and the equation can be approximated to

$$w(r) \approx -\frac{\pi C\rho_1\rho_2}{12}\left[\frac{1}{D^2}-\frac{1}{H^2}-\frac{1}{\delta^2}+\frac{1}{H^2}\right] = -\frac{\pi C\rho_1\rho_2}{12D^2}+\Delta, \quad (33)$$

where Δ is a constant.

As described by equation (8), at the critical point

$$x_{C3}^0\left(1-x_{5CB}^{critical}\right)U_{C3}-\Theta_{C3}W_{C3} = x_{5CB}^{critical}U_{5CB}-\Theta_{5CB}W_{5CB}. \quad (34)$$

Since C3 has very strong bonding (high desorption temperature) we assume that the coverage ratio of C3 is always 1. When the concentration of 5CB is high, the coverage ratio of 5CB is also close to 1. As a result we get

$$x_{C3}^0\left(1-x_{5CB}^{critical}\right)U_{C3}-W_{C3} = x_{5CB}^{critical}U_{5CB}-W_{5CB}, \quad (35)$$

$$x_{5CB}^{critical} = \frac{x_{C3}^0U_{C3}+W_{5CB}-W_{C3}}{x_{C3}^0U_{C3}+U_{5CB}} = 1+\frac{W_{5CB}-W_{C3}-U_{5CB}}{x_{C3}^0U_{C3}+U_{5CB}}. \quad (36)$$

Since U is in the form of $1/D^2$, let

$$U_{5CB} = \frac{\Psi_{5CB}}{D^2}+\Delta_{5CB}, \quad U_{C3} = \frac{\Psi_{C3}}{D^2}+\Delta_{C3}, \quad (37)$$

$$x_{5CB}^{critical} = \frac{x_{C3}^0U_{C3}+W_{5CB}-W_{C3}}{x_{C3}^0U_{C3}+U_{5CB}}$$
$$= \frac{x_{C3}^0\left(\frac{\Psi_{C3}}{D^2}+\Delta_{C3}\right)+W_{5CB}-W_{C3}}{x_{C3}^0\left(\frac{\Psi_{C3}}{D^2}+\Delta_{C3}\right)+\left(\frac{\Psi_{5CB}}{D^2}+\Delta_{5CB}\right)} \quad (38)$$
$$= \frac{x_{C3}^0\Psi_{C3}+\left(x_{C3}^0\Delta_{C3}+W_{5CB}-W_{C3}\right)D^2}{\left(x_{C3}^0\Psi_{C3}+\Psi_{5CB}\right)+\left(x_{C3}^0\Delta_{C3}+\Delta_{5CB}\right)D^2}.$$

It is easy to see that x is in the form of

$$x_{5CB}^{critical} = \frac{1}{\xi+\gamma D^2}+\varphi, \quad (39)$$

where γ, φ and ξ are all positive invariants to SiO_x thickness.

From Equation (39) we know when the thickness of SiO_x increases, the critical concentration of 5CB should decrease. The physical meaning of this effect can be understood in the following way. At the point of the transition 5CB has a concentration of over 50% and we assume the surface is saturated with absorbed 5CB molecules. Further, we have confirmed in our experiments that the dielectric anisotropy of the mixture becomes positive when the concentration of 5CB is higher than 33%. Van der Waals potential would prefer planar alignment but surface short range interaction prefers vertical alignment. With the increase of SiO_x thickness more van der Waals potential is gained to compete with the same amount of short-range interactions. Therefore, less 5CB (smaller $\Delta\varepsilon$) is needed to cause the transition due to the greater polarisation of the surface for thicker SiO_x. Experimental data has been fitted using Equation (39), as shown in Figure 17.

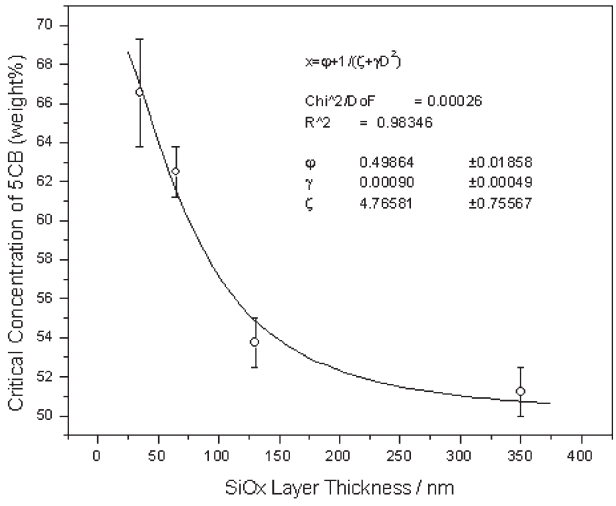

Figure 17. The critical concentration of 5CB in the homeotropic-to-planar anchoring transition of 5CB/LC1 mixtures depends on the thickness of underlying SiO_x layer.

Screening effect.

Because of its "long range" nature, van der Waals force originating from SiO_x can be "felt" by LC molecules even if they are separated by intermediate polyimide layers. PI 7511L is known to promote perpendicular alignment on its surface. But the preference of SiO_x underneath depends on the dielectric anisotropy of the LC. For 5CB, which has a positive $\Delta\varepsilon$, the long-range van der Waals interaction would prefer planar alignment, which is different from the perpendicular alignment favoured by PI 7511. Therefore anchoring transitions between homeotropic and planar alignment can take place when the relative strength of long-range and short-range interactions changes. In Figure 13(a) we have shown that with a fixed polyimide thickness, increasing the SiO_x thickness shifted the anchoring towards planar.

We interpret this as the result of the van der Waals potential (that prefers planar alignment) being strengthened. In contrast, in Figure 13 b we observed anchoring transitions due to the increased short-range surface interactions resulting from the increased PI thickness. The experimental data therefore fit with our theory.

On the other hand, MLC-6609 has a negative $\Delta\varepsilon$ so the long-range van der Waals interaction between SiO_x and LC prefers homeotropic alignment, which agrees with short-range forces between PI 7511 and the LC materials. Hence, no anchoring transition was observed in the experiments.

Difference in surface properties between SiO_x and SiO_2, and the effect on anchoring

As discussed in previous sections, we propose an explanation of the alignment of a LC on LAD-SiO_x in terms of the competition between long-range van der Waals torque and short-range dipolar torques. Changes in surface properties can lead to changes in the strength of short-range interaction and therefore cause anchoring transitions.

SiO_x has an unsaturated structure. From the XPS data we know that even on the surface of the SiO_x layer the ratio between oxygen atoms and silicon atoms is significantly smaller than 2. This leads us to believe that there are a lot of *dangling bonds* on the SiO_x surface, which tend to interact strongly with the dipole moments of LC molecules. On the other hand, e-beam evaporated SiO_2 shows a well-saturated stoichiometry. Therefore we should expect a more passive surface that is less polar and interacts less with polar LC molecules. As a result, LC1 (which contains high concentration of materials with large lateral dipole moment) assumes parallel anchoring on SiO_x but perpendicular on SiO_2. Figure 14 shows the anchoring transition from perpendicular to planar when C3 is added into LC2. The critical concentration of C3 needed to trigger the anchoring transition is much higher on SiO_2 than on SiO_x. This is also because e-beam evaporated SiO_2 has less surface polarity than thermally evaporated SiOx, meaning the short range surface dipolar interactions (that prefer parallel anchoring) between SiO_2 and C3 is also smaller than that between SiO_x and C3. Therefore more C3 is needed for SiO_2 to achieve the same magnitude of short-range torque on SiO_x to compete with long range van der Waals torque.

5. Conclusion

We have observed anchoring transitions on SiO_x caused by the addition of two kinds of additives, one that has a large longitudinal dipole and the other having a large lateral dipole moment. The anchoring transitions were found to be dependent on temperature and SiO_x thickness.

We propose that the discovered aspects of LC alignment on LAD-SiO_x can be explained as a result of competition between long-range van der Waals interaction and short-range dipolar interactions, which have an opposite preference in the anchoring direction. This explanation fits with a wide range of observed data, including the concentration dependence of additives that have longitudinal and lateral dipoles, the temperature dependence and the effect of surface layer thickness.

Acknowledgements

The authors would like to thank HANA Microdisplay Technology Inc for sponsoring the research. Our colleagues Liou Qiu and Dr. Oleg Lavrentovich have helped us with the AFM study. Dr. Quan Li and Julie Kim helped us to synthesis compounds we needed. Dr. Robert Twieg and Dr. Alexander Semyonov helped us with GCMS. Also, Dr. Gail Harkey at Thermo Electron Corp. provided help in the TDMS experiments. Dr. Wayne Jennings at Case Western Reserve Univ. helped us with the XPS study. We would like to express our thanks to all of them.

References

(1) Heffner W.R.; Berreman D.W.; Sammon M.; Meiboom S. *Appl. Phys. Lett.* **1980**, *36*, 144.
(2) Urbach W.; Boix M.; Guyon E. *Appl. Phys. Lett.* **1974**, *25*, 479.
(3) Kahn F.J. *Appl. Phys. Lett.* **1973**, *22*, 386.
(4) Wen C.-H.; Gauza S.; Li J.; Wang H.; Wu S.-T. *Liq. Cryst.* **2005**, *32*, 643.
(5) Kubono A.; Onoda H.; Inoue K.; Tanaka K.; Akiyama R. *Mol. Cryst. liq. Cryst.* **2002**, *373*, 127.
(6) Uchida T.; Watanabe H.; Wada M. *Jap. J. appl. Phys.* **1972**, *11*, 1559.
(7) Perez E.; Proust J.E.; Ter-Minassian-Saraga L. *Mol. Cryst. liq. Cryst.* **1977**, *42*, 167.
(8) Dubois-Violette E.; de Gennes P.G.J. Phys. Lett. **1975**, *36*, 255.
(9) Dubois-Violette E.; de Gennes P.G.J. Colloid Interface Sci. **1976**, *57*, 403.
(10) Sonin A.A. *The Surface Physics of Liquid Crystals*; Gordon and Breach: **1995**. pp. 118–127.
(11) Yokoyama H. *Mol. Cryst. liq. Cryst.* **1988**, *165*, 265.
(12) Smith E.R.; Ninham B.W. *Physica* **1973**, *66*, 111.
(13) Bernasconi J.; Strassler S.; Zeller H.R. *Phys. Rev. A* **1980**, *22*, 276.
(14) Lu M.; Yang K.H.; Nakasogi T.; Chey S.J. *SID Intl. Symp. Dig.* **2000**, *29*, 446.
(15) Vithana H.; Johnson D.; Bos P. *Jap. J. appl. Phys.* **1996**, *35*, 320.
(16) Kang H.-K.; Hwang J.-Y.; Park C.-J.; Seo D.-S.; Kim K.-C.; Ahn H.-J.; Kim J.-B.; Baik H.-K. *Mol. Cryst. liq. Cryst.* **2005**, *434*, 135.
(17) Blinov L.M.; Sonin A.A. *Langmuir* **1987**, *3*, 660.

(18) Blinov L.M.; Sonin A.A. *Mol. Cryst. liq. Cryst.* **1990**, *179*, 13.
(19) Guyon E.; Pieranski P.; Boix M. *Lett. appl. Engng Sci.* **1973**, *1*, 19.
(20) Berreman D.W. *Phys. Rev. Lett.* **1972**, *28*, 1683.
(21) Wilson T.; Boyd G.D.; Westerwick E.H.; Storz F.G. *Mol. Cryst. liq. Cryst.* **1983**, *94*, 359.
(22) Goodman L.A.; Mcginn J.T.; Anderson C.H. *IEEE Trans. Electron. Dev.* **1977**, *24*, 795.
(23) Papanek J.; Martinot-Lagarde P. *J. Phys., Paris II* **1996**, *6*, 205.
(24) Wagendristel A.; Wang Y. *An Introduction to Physics and Technology of Thin Films*; World Scientific: Singapore, 1994.
(25) Monkade M.; Martinot-Lagarde P.; Durand G.; Granjean C. *J. Phys., Paris II* **1997**, *2*, 1577.
(26) Philipp H.R. *J. Phys. Chem. Solids* **1971**, *32*, 1935.
(27) Philipp H.R. *J. non-crystalline Solids* **1972**, *8–10*, 627.
(28) Hohl A.; Wieder T.; van Aken P.A.; Weirich T.E.; Denninger G.; Vidal M.; Oswald S.; Deneke C.; Mayer J.; Fuess H. *J. non-crystalline Solids* **2003**, *320*, 255.
(29) Reznikov Y.; Ostroverkhova O.; Singer K.D.; Kim J.-H.; Kumar S.; Lavrentovich O.; Wang B.; West J.L. *Phys. Rev. Lett.* **2000**, *84*, 1930.
(30) Katsten H.; Strobl G. *J. chem. Phys.* **1995**, *103*, 6768.
(31) Meiboom S.; Sammon M. In *The Physics and Chemistry of Liquid Crystal Devices*; Sprokel G.J. (Ed.), Plenum: New York, 1980. p. 13.
(32) Van Hom B.L.; Winter H.H. *Appl. Opt.* **2001**, *40*, 2089.
(33) Uchida T.; Seki H. In *Liquid Crystal: Applications and Uses*, Vol. 3, Bahadur B. (Ed.), World Scientific: 1992, Chapter 5, p. 36.
(34) Shimoda S.; Mada H.; Kobayashi S. In *Physics of Liquid Crystal Devices*; Sprokel G.J. (Ed.), Plenum: New York, 1980. pp. 47–60.
(35) Hiroshima K.; Mochizuki M. *Jap. J. appl. Phys.* **1978**, *19*, 567.
(36) van Sprang H.A.; Aartsen R.G. *J. appl. Phys.* **1984**, *56*, 251.
(37) Graf K.; Butt H.-J.; Kappl M. *Physics and Chemistry of Interfaces*; Willey-VCH; Chapter 9, p. 185.
(38) Israelachvili J. *Intermolecular and Surface Forces*, 2nd ed., Academic Press: 1991, Chapter 10, p. 155.